The influences of the AMO and NAO on the sedimentary infill in an Azores archipelago lake since ca. 1350CE

Armand Hernández, Alberto Sáez, Roberto Bao, Pedro M. Raposeiro, Ricardo M. Trigo, Sara Doolittle, Pere Masqué, Valentí Rull, Vítor Gonçalves, David Vázquez-Loureiro, María J. Rubio-Inglés, Guiomar Sánchez-López, Santiago Giralt

PII: S0921-8181(17)30007-3
DOI: doi: 10.1016/j.gloplacha.2017.05.007
Reference: GLOBAL 2590

To appear in: *Global and Planetary Change*

Received date: 7 January 2017
Revised date: 26 May 2017
Accepted date: 29 May 2017

Please cite this article as: Armand Hernández, Alberto Sáez, Roberto Bao, Pedro M. Raposeiro, Ricardo M. Trigo, Sara Doolittle, Pere Masqué, Valentí Rull, Vítor Gonçalves, David Vázquez-Loureiro, María J. Rubio-Inglés, Guiomar Sánchez-López, Santiago Giralt , The influences of the AMO and NAO on the sedimentary infill in an Azores archipelago lake since ca. 1350CE, *Global and Planetary Change* (2017), doi: 10.1016/j.gloplacha.2017.05.007

The influences of the AMO and NAO on the sedimentary infill in an Azores Archipelago lake since ca. 1350 AD

Armand Hernández[1,2], Alberto Sáez[3], Roberto Bao[2], Pedro M Raposeiro[4], Ricardo M. Trigo[1], Sara Doolittle[2], Pere Masqué[5,6,7], Valentí Rull[8], Vítor Gonçalves[4], David Vázquez-Loureiro[2], María J Rubio-Inglés[8], Guiomar Sánchez-López[8], Santiago Giralt[8]

1 Instituto Dom Luiz (IDL), Faculdade de Ciências, Universidade de Lisboa, 1749 016 Lisboa, Portugal

2 Centro de Investigacións Científicas Avanzadas (CICA). Facultade de Ciencias, Universidade da Coruña, 15071 A Coruña, Spain

3 Department of Earth and Ocean Dynamics. Faculty of Earth Sciences. Universitat de Barcelona. Marti i Franques s/n. 08028 Barcelona, Spain

4 CIBIO, Centro de Investigação em Biodiversidade e Recursos Genéticos, InBIO Laboratório Associado, Pólo dos Açores – Departamento de Biologia da Universidade dos Açores, 9501-801 Ponta Delgada, Portugal

5 School of Science. Edith Cowan University. 270 Joondalup Drive, Joondalup WA 6027. Australia

6 Departament de Física & Institut de Ciència i Tecnologia Ambientals. Universitat Autònoma de Barcelona. 08193 Bellaterra. Spain

7 Oceans Institute & School of Physics. The University of Western Australia. 35 Stirling Highway. Crawley, WA 6009. Australia

8 Institute of Earth Sciences Jaume Almera (ICTJA-CSIC), Lluís Solé i Sabarís s/n, E-08028 Barcelona, Spain

*Correspondence to:
Armand Hernández
Instituto Dom Luiz (IDL), Faculdade de Ciências, Universidade de Lisboa, 1749-016 Lisboa, Portugal.
Phone: +351 217 500 863
Fax: +351 217 500 977
E-mail: ahhernandez@fc ul pt

Abstract

The location of the Azores Archipelago in the North Atlantic makes this group of islands an excellent setting to study the long-term behavior of large oceanic and atmospheric climate dynamic patterns, such as the Atlantic Multidecadal Oscillation (AMO) and the North Atlantic Oscillation (NAO). Here, we present the impacts of these patterns on Lake Empadadas (Azores Archipelago) from the Medieval Climate Anomaly (MCA) - Little Ice Age (LIA) transition to the present based on sedimentological, geochemical and biological characterizations of the sedimentary record. Multivariate analyses of a number of proxies including X-ray fluorescence (XRF), X-ray diffraction (XRD), total organic and inorganic carbon (TOC and TIC) and diatom life forms abundance reveal that the sedimentary infill evolution has been controlled by (i) fluctuations in the lake level and (ii) variations in organic matter accumulation. Both processes are governed by climate variability and modulated by anthropogenic activities associated with changes on the lake catchment. Changes in these two sedimentary processes have been used to infer five stages: (i) the MCA-LIA transition (ca. 1350-1450 AD) was characterized by a predominantly positive AMO phase, which led to intermediate lake levels and high organic matter concentration; (ii) the first half of the LIA (ca. 1450 - 1600 AD) was characterized by predominant lowstand conditions and intermediate organic matter deposition mainly related to negative AMO phases; (iii) the second half of the LIA (ca. 1600 - 1850 AD) was characterized by negative AMO and NAO phases, implying intermediate lake levels and high organic matter deposition; (iv) the Industrial era (ca. 1850 – 1980 AD) was characterized by the lowest lake level and organic matter accumulation associated with negative AMO phases; and (v) the period spanning between 1980 AD and the present reveals the highest lake levels and low organic matter deposition, being associated with very positive AMO conditions. At decadal-to-centennial scales, the influence of the AMO on Azorean climate plays a larger role than previously thought. In fact, the AMO appears to exert a stronger influence compared to the NAO, which is the main mode of climate variability at shorter time scales.

Keywords: Climate modes; Paleoclimatology; Paleolimnology; Oceanic Islands; Last millennium

1.- Introduction

Small and remote islands are very sensitive and vulnerable to environmental changes, and their limited area and resources can complicate adaptation policies (IPCC, 2014; Nurse et al. 2014). Thus, there is a growing interest in predicting the environmental consequences of ongoing and future global changes in areas of land surrounded by large water masses. With few exceptions (e.g., Cropper and Hanna, 2014; Hernández et al., 2016), the instrumental climate records from remote islands are limited to the 20th century; therefore, it is necessary to extend climatic reconstructions using paleoclimatic proxy data to i) establish the background conditions before the current global change, ii) investigate previous periods characterized by notable climatic shifts attributable to natural forcing and widespread human activities, and iii) comprehend the environmental impacts of these climate changes. Despite the fact that small oceanic islands are exceptional locations to study the impacts of large oceanic and atmospheric climate patterns, only a few high-resolution terrestrial paleoenvironmental records from these islands exist (e.g., Björck et al., 2006; Conroy et al 2008; Margalef et al., 2013). Consequently, appropriate high-resolution paleoarchives are required to improve the understanding of recent climate variability and its impacts (PAGES 2K Consortium, 2013; Jones et al., 2009)

Three main climate periods within the last millennium have been clearly identified: the Medieval Climate Anomaly (MCA; ca. 800 – 1400 AD), the Little Ice Age (LIA; ca. 1400 – 1800 AD) and the Industrial era (ca. 1850 AD-Present). There is a general consensus defining the MCA and Industrial era as warm periods and the LIA as a cooler period (Mann et al., 2009). Several works have focused on the main driving mechanisms behind these anomalies and their transitions. The main mechanisms driving the climate cooling during the LIA have been linked to two major external forcing factors, solar activity and volcanism. The cooling has primarily been attributed to the decrease of incident solar radiation on the Earth's surface (Shindell et al., 2001; Solanski et al., 2004; Vaquero and Trigo, 2015) and to stronger volcanic activity (Bradley and Jones, 1992; Fischer et al., 2007). The effect of these external forcings was probably amplified by responses from the oceanic component of the climate system, particularly by the slowdown of the North Atlantic thermohaline circulation (Broecker, 2000). Overall, these assessments point to the previous natural external forcings that resulted in a prolonged reinforcement of ocean-atmosphere positive feedback mechanisms (Trouet et al., 2012). New promising studies highlight the relevance of atmospheric patterns affecting the climate conditions over the North Atlantic sector during these periods (e.g., Moffa-Sánchez et al. 2014; Sánchez-López et al. 2016)

The climate variability in the North Atlantic sector is influenced by a number of large-scale patterns or modes of climate variability (e.g., Marshall et al., 2001; Trigo et al., 2004), which affect the environment and society in multiple ways (e.g., Ottersen et al. 2001; Jerez and Trigo, 2013). The North Atlantic Oscillation (NAO) is the leading mode of atmospheric circulation variability over this region, and it is defined as the atmospheric pressure difference between the Icelandic Low and the Azores High (e.g., Hurrell, 1995; Hurrell et al., 2003). In addition to the NAO, the Atlantic Multidecadal Oscillation (AMO;

Mann et al., 2009) is another mode of natural variability in this area. The AMO has been identified as a coherent pattern of oscillatory changes in North Atlantic sea-surface temperatures at multidecadal time scales (e.g., Sutton and Hodson, 2005; Mann et al., 2009). In the Azores Archipelago, both the NAO and the AMO have recently been recognized as the main large-scale patterns that exert a discernible influence on the climate regime of the Azores Archipelago at interannual time scales (Hernández et al., 2016). These modes can affect and control different mechanisms (i.e., tropical cyclones, convection, thunderstorms, frontal passages, sea surface temperature anomalies and jet streams) that bring moisture responsible for several phenomena (e.g., Kossin et al., 2010). However, their combined influence on these islands at different time scales remains unclear beyond the instrumental period.

Here, we present new insights into the environmental evolution of Lake Empadadas (Azores Archipelago) since ca. 1350 AD by means of a high-resolution multi-proxy study of its sedimentary sequence. Sedimentological, biological and geochemical data are employed to reconstruct fluctuations in the water level, the organic matter (OM) accumulation and the changes in the vegetation covering the catchment. We seek to disentangle the combined influences of the NAO and AMO on the studied lake system during the last centuries. To the best of our knowledge, this study is the first to assess the impact of decadal-to-centennial climate variability on a lake that takes into account these two major North Atlantic climate modes

2.- Study site

The Azores Archipelago (37°- 40° N, 25°- 31° W) comprises nine islands and several islets in the North Atlantic Ocean (Fig. 1A). These islands are of volcanic origin, having risen along sea-floor fracture zones as the Eurasian, African and North American tectonic plates rifted apart (Azevedo and Ferreira, 2006). At the western part of São Miguel Island, Lake Empadadas Norte (37º49’ N - 25º45’ W) occupies the bottom of a small crater that is 740 m above sea level (Fig. 1B). Its maximum length and width are 250 m and 85 m, respectively, and its maximum water depth is 5.3 m. The total area of the lake is 0.02 km^2, its total water volume is $3.7x10^4$ m^3, and the total area of the catchment is 0.10 km^2 (Porteiro, 2000). The lake is polymictic with a pH ranging between 6.24 and 7.62, very low conductivity (16.7 – 33.9 $\mu S\ cm^{-1}$) and low mineralization (22.5 – 36.7 $mg\ l^{-1}$), and its chemistry is dominated by Na^+ and Cl^- (Cruz et al., 2006; Pereira et al., 2014).

The Sete Cidades volcanic complex, in which Lake Empadadas is located (Fig. 1), was formed by a basaltic injection into a trachytic magma chamber approximately 210,000 yr BP (Moore, 1991). Three major phases of volcanic activity occurred: i) pre-caldera, ii) caldera consolidation and iii) post-caldera. The last period featured a sequence of explosive eruptions producing trachytic volcaniclastic deposits and pyroclastic flows that led to the collapse of the caldera (Moore, 1991). The oldest eruption was dated to 210,000±8000 yr BP, whereas the youngest eruption (P17) was dated to 663±105 yr BP (Shotton and Williams, 1971) and 500±100 yr BP (Moore and Rubin, 1991). After this date, only

volcaniclastic deposits from historic eruptions of other volcanic complexes (e.g., Furnas and Fogo) are found in the Sete Cidades area (Madeira, 2007).

The climate in the Azores Archipelago is temperate oceanic and characterized by mild temperatures with small annual variations, a rainfall regime that displays a strong seasonal cycle and large interannual variability, high relative air humidity, generally cloudy skies, and frequent strong winds (Hernández et al., 2016). The climatic conditions are determined by the strength and position of the Azores Current (a branch of the Gulf Stream) and the semi-permanent high-pressure Azores Anticyclone (Volkov and Fu, 2010). Between September and March, if the high-pressure center is dissipated or displaced, the Azores region is frequently crossed by the North Atlantic storm-track, the main path of rain-producing weather systems. Conversely, during late spring and summer, the Azores climate is mainly dominated by the Azores Anticyclone (Santos et al., 2004). A large fraction of the seasonal and interannual climate variability observed in the Azores Archipelago has been ascribed to the NAO influence (Andrade et al., 2008; Cropper and Hanna, 2014; Hernández et al., 2016). However, when the NAO influence becomes weaker, the effects of other large-scale modes appear to increase, highlighting the non-stationary influences of these modes on Azorean climate (Hernández et al., 2016). In particular, at decadal and longer time scales the AMO is also a relevant mode of natural variability in this area (Yamamoto and Palter, 2016). Temperature is positively correlated with both the NAO and AMO, whereas precipitation is negatively correlated with the NAO and positively correlated with the AMO (Mann et al., 2009; Cropper and Hanna, 2014; Hernández et al., 2016).

3.- Materials and methods

In September 2011, five sediment cores (up to 2.7 m long) were retrieved from Lake Empadadas using an UWITEC® piston corer installed in an UWITEC® platform raft. All cores were split longitudinally into two halves and imaged with a high-resolution color line scan camera. This study focused on the longest and best preserved core (EMN11-04) retrieved from the offshore zone of the lake (Figs. 1 and 2). Sedimentary facies were defined and characterized by visual recognition assisted by microscopic smear slide observations every cm and the results of geochemical and mineralogical analyses.

The age model was constructed using the concentration profile of ^{210}Pb coupled with ^{14}C dating of terrestrial plant macroremains. The well-known date of the last volcanic eruption was also used as a tie point. ^{210}Pb was measured in the uppermost 40 cm of the core. These analyses were conducted at the Environmental Radioactivity Laboratory of the Universitat Autònoma de Barcelona. Sedimentation rates were determined using the Constant Flux:Constant Sedimentation (CF:CS) model (Robbins, 1978). Concentrations of ^{210}Pb were determined through the analysis of its granddaughter ^{210}Po by alpha-spectroscopy, assuming secular equilibrium of both radionuclides at the time of analysis (Sánchez-Cabeza et al. 1998). A known amount of ^{209}Po was added to each sample as internal tracer. Samples were acid digested using an analytical microwave, solutions were conditioned in HCl 1N and polonium isotopes were plated onto silver discs. Alpha

emissions were measured using Passivated Implanted Planar Silicon (PIPS) detectors (CANBERRA, Mod. PD-450 18 A M) and the activities quantified after corrections for background and reagent blanks. Supported ^{210}Pb concentrations were determined by averaging the total ^{210}Pb concentrations at the base of the ^{210}Pb profile, verified with some measurements of ^{226}Ra concentrations along the core carried out by gamma-spectroscopy using a high-purity germanium detector (CANBERRA, mod. GCW3523). AMS ^{14}C dates of four samples were obtained by Beta Analytic Inc. Laboratory (USA) (Table 1). The radiocarbon ages were calibrated to calendar years (cal AD) using the CALIB 7 1 software (Stuiver and Reimer, 1993) and the INTCAL13 curve (Reimer et al., 2013), selecting the median of the 95.4 % distribution (2σ probability interval) (Table 1). Finally, the EMN11-04 age-depth model (Fig. 3), including the ^{210}Pb-derived and ^{14}C-derived ages, was constructed using the mixed effect regression method (Heegaard et al., 2005). For this purpose, the uppermost and lowermost ^{210}Pb-derived ages were converted to radiocarbon dates. Once the age-depth model was constructed, the ages of the samples were converted to AD ages

The best preserved half of each section of the studied core was analyzed using X-ray fluorescence (XRF) with the AVAATECH XRF II core scanner at the Universitat de Barcelona (Spain). The XRF measurements were performed every 2 mm where the material was well preserved (i.e., from top to bottom: 0-24 cm, 118.5-148.5 cm, 167.5-213 cm and 218-237.5 cm). Among the thirty-two chemical elements tested for, only 9 elements (Al, Si, K, Ca, Ti, Mn, Fe, Sr and Zr) had sufficient intensity (counts per second) to be considered statistically significant

For mineralogical analyses, the core was sampled every cm in the following intervals: 0 to 33 cm, 58 to 62 cm, 87.5 to 100.5 cm, 114.5 to 162.5 cm, and 165.5 to 237.5 cm. Samples in between these ranges were not considered because they were not of lacustrine origin. All the samples were dried at 60 °C for 48 h and were manually ground using an agate mill. Mineralogical analyses were conducted using X-ray diffraction (XRD) with a SIEMENS-D500 automatic X-ray diffractometer (Cu-Kα, 40 kV, and 30 mA) and a graphite monochromator at the Institute of Earth Sciences Jaume Almera (ICTJA-CSIC, Spain). The XRD patterns revealed that the samples were composed of two fractions: a crystalline fraction (highlighted by different peaks) and an amorphous fraction (characterized by the presence of a broad peak centered at 20 - 25º 2θ). The identification and quantification of the relative abundances of the different mineralogical species present in the crystalline fraction were conducted following the standard procedure based on the matrix-flushing theory (Chung 1974 a, b). The amorphous fraction percentage was estimated by calculating the area of the broad 20 - 25º 2θ peak using the EVA software installed on the X-ray diffractometer and diagrams for quantification using smear slide observations (Terry and Chillingar, 1955; Kienel et al., 2005)

The samples for XRD analysis were also employed for total carbon (TC) and total nitrogen (TN) analyses (relative standard deviation = 0.05). These analyses were carried out using a Finnigan delta Plus EA-CF-IRMS spectrometer at the laboratories of the Centres Científics i Tecnològics of the Universitat de Barcelona. The carbonate content

was below the detection limit of the X-ray diffractometer, and consequently, the TC was considered equal to the total organic carbon (TOC). The TOC/TN atomic ratio was also calculated for all the samples. The fluxes of TOC into the sediments were estimated as mass accumulation rates (MARs) by multiplying the TOC concentration by the sediment dry density and sedimentation rate at each depth.

The statistical treatment of the data was performed using R software (R Development Core Team, 2015). As stated before, and since the XRF data was originally at 2 mm resolution, they were calculated with a regular spacing of 10 mm using the R function 'approxTime' to obtain the same spatial resolution to conduct the statistical analyses for all proxies. The environmental stages were identified by means of stratigraphically constrained cluster analysis (CONISS) and the statistically significant stages were selected using the broken-stick model (Bennett, 1996). Principal Component Analysis (PCA) and Redundancy Data Analysis (RDA) were performed after standardizing and resampling the dataset with a regular spacing of one cm and omitting rows with missing values. RDA was performed to identify the provenances of the XRF-determined elements and the OM. The mineralogical composition of the sediments was used as a constraining matrix, given that each mineralogical species represents a “compendium” of geochemical elements (Giralt et al., 2008). In turn, the PCA was employed to extract the main components of variability in the XRF and OM datasets. A dataset of 13 variables and 117 samples was created to apply the PCA and RDA. Despite their non-lacustrine origin, four samples from tephra layers were included in the multivariate analysis as passive data points to help in the identification of the composition and origin of the amorphous fraction of the sediments.

Instrumental records (1872-2012) of precipitation (Hernández et al., 2016) and temperature (Cropper and Hanna, 2014) were obtained from the Ponta Delgada Station (São Miguel Island, Azores Archipelago). The extended daily (1850 to present) station-based NAO index by Cropper et al. (2015), as well as the AMO index from 1856 to the present from the NOAA (https://www.esrl.noaa.gov/psd/data/timeseries/AMO/)have been employed for the instrumental period.

Spearman's rank correlation coefficients (ρ) and associated p-values were also applied to assess the impact of the large-scale modes of climate variability and the meteorological variables on the limnological variability for the instrumental period (1873-2011) at the decadal scale according to the chronological model. The mean values of each instrumental variable during the years estimated to be included in each sediment sample, according to the available age model, were considered. No significant autocorrelation was observed for any variable. The datasets were also detrended and the subsequent spectral analyses did not reveal any significant periodicity (not shown). The Bonferroni correction was carried out to establish a significant threshold (Hochberg, 1988), and thus, unless otherwise stated, significance (p-value) is always discussed at p<0 01

4.- Results and interpretations

4.1.- Chronology

The concentration profile of ^{210}Pb in the EMN11-04 core shows three distinct zones: 0 - 13 cm, 13 – 30 cm, and >30 cm. Based on the CF:CS model, the sedimentation rate is 2 ± 0 7 cm yr^{-1} in the first zone interval (0 – 13 cm) and 0 43 ± 0 04 cm yr^{-1} in the second interval (13 – 30 cm). The chronologies of these two intervals cover the period from 2011 to 1965 AD. The concentrations of ^{210}Pb below 30 cm are compatible with the supported ^{210}Pb because they are in equilibrium with the ^{226}Ra values measured by gamma spectrometry in selected samples; thus, it is not possible to obtain reliable ages (Figure 1S Supplementary Material)

The four AMS ^{14}C dates from the EMN11-04 core are stratigraphically coherent and feature no reversals. Therefore, all the radiocarbon dates are included in the construction of the age-depth model (Figure 3 and Table 1). The lowest date (236 5 cm; 630 ± 30 cal yr BP) almost corresponds with the bottom of the lacustrine sequence (238 5 cm), and it overlies the tephras of Unit 1. As stated in the next section, Unit 1 most likely corresponds to the P17 volcanic eruption episode, making us suspect that 663±105 yr BP date (Shotton and Williams, 1971) is more likely than 500±10 yr BP (Moore and Rubin, 1991). Moreover, similar AMS ^{14}C date obtained in Lake Azul over P17 tephra Unit reinforced this hypothesis (Raposeiro et al., 2017; Rull et al. 2017).

The age model was calculated without taking into account the thickness of intervals composed of non-lacustrine deposits (see the next section for further information) because they accumulated via instantaneous sedimentary processes (Figs. 2 and 3). Hence, according to the age model, core EMN11-04 spans from ca. 1350 AD to 2011 AD (Fig. 3 and Table 1). The mean sedimentation rate is 0.2 mm yr^{-1} between core depths of 250 and 160 cm, and it increases to a mean value of 0.6 mm yr^{-1} from 160 cm to the top of the record.

4.2.- Sedimentary units and facies description

The following five sedimentary units composed of six lacustrine facies have been defined based on textural, biological, geochemical and mineralogical features of the sediments in the EMN11-04 core.

4.2.1.- Unit 1 (bottom to 239 cm depth; ca. 1350 AD)

Unit 1 contains gray to white volcaniclastic deposits composed of coarse lapilli material interbedded with layers of fine ash particles (Facies T) with scarce biological elements (e.g., diatoms, chironomids, macrophytes). The layers dip to a certain degree. The presence of rare lacustrine flora indicates that the volcanic material accumulated directly in the lake by fallout transport. Taking into account the age of the overlaying sediments, the volcanic deposits of this unit likely correspond to the P17 volcanic eruption (Queiroz et al., 2008)

4.2.2.- Unit 2 (239 to 214 cm depth; ca. 1350 to 1450 AD)

The sediments in Unit 2 were deposited unconformably on top of Unit 1. Unit 2 is composed of massive dark-brown organic-rich lacustrine muddy sediments with

macrophyte remains and dispersed sand grains (Facies A). Smear slide observations revealed a dominance of tychoplanktonic diatoms belonging to colonial genera of *Fragilaria* s l. group, a high concentration of chironomid head capsules, and some phytoliths. This unit displays the highest percentages of TOC, TN and TOC MARs of the record (Fig. 4). The TOC/TN atomic ratio oscillates between 12 and 23. The observed presence of rare terrigenous materials (only significant amounts of coarse particles) corresponds with the low XRF signal of this facies (Fig. 5). The XRD analyses indicate a significant amorphous fraction (~80 % of the total) composed of a mixture of biogenic silica, OM and, to a lesser extent, volcanic glass. The mineral crystalline fraction is mainly composed of sanidine and plagioclase and secondarily by quartz and illite. This unit presents the highest quartz content of the entire record, with mean values around ~15 % of the crystalline fraction

In offshore zones of small lakes, organic-rich mud with plant remains and a dominance of tychoplanktonic diatoms usually corresponds to deposits accumulated in shallow perennial water table conditions (Kingsbury et al., 2012). Moreover, the high TOC/TN ratios indicate that the high amounts of accumulated OM originated by the development of abundant macrophytes and external inputs (Figure 2S Supplementary Material).

4.2.3.- Unit 3 (214 to 166 cm depth; ca. 1450 to 1850 AD)

Unit 3 is mainly composed of banded brown mud and silt (Facies B). Diatoms and chironomid head capsules are less abundant than in Unit 2, whereas this unit is richer in phytoliths and fine/altered terrigenous particles. The diatom assemblage is dominated by benthic life forms, mainly *Cymbella* s l. taxa, particularly in the lower part of the unit, indicating low lake levels (Figure 2S Supplementary Material). This unit shows lower values of %TOC, TOC MARs and %TN than Unit 2 (Fig. 4). It also shows a lower TOC/TN ratio (Fig. 4), with values of approximately 13, most likely due to the lower abundance of macrophytes. The higher illite and lower quartz contents in this unit might be related to the erosion of soils formed on volcanic rocks during lake lowstand conditions, resulting in the transport of only clay particles to the center of the lake. The estimated amorphous fraction represents approximately 80 % of the total sample and is dominated by a very high proportion of volcanic glass, as indicated by both the smear slides and the high XRF values (Fig. 5). The main components of the crystalline fraction are sanidine and plagioclase

The upper part of this unit (195-166 cm depth; ca. 1600 to 1850 AD) recorded an increase in tychoplanktonic diatoms (*Fragilaria* s l ; Fig. 4). Higher quartz and lower illite contents were also observed (Fig. 5), possibly due to intensified runoff that might have triggered a lake level rise and the flooding of previously exposed areas along the lake margin. In turn, smaller amounts of amorphous materials but higher TOC and TN contents and slightly lower TOC/TN values than those between 214 cm and 195 cm (Fig. 4) indicate the greater accumulation of OM with an algal origin.

Additionally, two fine-grained tephra layers corresponding to ash flow deposits (Facies T) were identified between the muddy and silty sediments (Facies B) of this unit (Fig. 2). These tephra deposits likely correspond to secondary volcanic episodes from the historic eruptions of the Furnas (1439/44 AD) and Fogo (1563 AD) volcanic complexes (Madeira, 2007). Between 165 and 150 cm core depth, a disorganized and non-erosive gravel interval interrupted the lacustrine sedimentation (Fig. 2). The sedimentological features (i.e., high textural heterogeneity, absence of matrix and biological remains, and non-erosive contacts) and the date of the deposition (ca. 1850 AD) suggest an anthropogenic origin probably related to human activities in the lake catchment (Moreira, 1987; Rull et al., 2017)

4.2.4.- Unit 4 (150 to 114 cm depth; ca. 1850 to 1980 AD)

Unit 4 is composed of bands of dark- to pale-brown silts (Facies C) interbedded with a sand layer (Facies S). The band thickness of Facies C varies between 1 and 5 cm. Chironomid head capsules and diatom contents are the lowest of the whole record, with a dominance of benthic diatoms (mainly genera belonging to *Cymbella* s.l. and *Pinnularia* s.l.), suggesting very shallow lake levels and a non-perennial water table (Fig. 6). The TOC and TN values are fairly constant and are also the lowest of the whole record (Fig. 4). The TOC MARs and the TOC/TN values are low but are similar to those of Unit 3, indicating a predominantly aquatic algal origin of the scarce accumulated OM (Fig. 4). The estimated amorphous fraction is lower (<80 %) than in facies A and B. This facies is mainly made up of tephra particles (high XRF values), especially in the dark bands, which display higher XRF values than the pale bands (Fig. 5). The crystalline fraction is dominated by illite, with sanidine and plagioclase as secondary components, whereas the quartz fraction is the lowest of the entire record. This high content of volcanic glass and illite supports the interpreted lowstand conditions with the input of soil particles that formed on the unflooded lake margins and were transported to the center of the lake. It is worth noting that the pale bands are richer in diatoms, whereas the dark ones are richer in OM and coarse particles

Facies S, represented by a single ~2-cm-thick layer, consists of coarse sand embedded in a matrix of medium sand and silt. Grains of quartz, plagioclase, clay minerals and tephra are the dominant components, and they are similar to those of the organic facies. In this layer, the mineral content is much higher than the OM, and the diatom valve concentration is very low. The diatom assemblage is mainly composed of benthic diatoms, with *Cymbella* s l. being the dominant group. These sedimentary features might indicate an extraordinary flood event that occurred at approximately 1890 AD

From 115 to 33 cm core depth, a disorganized gravel layer lies between lacustrine sediments and shows no signs of erosion (Fig. 2). Again, the sedimentological features (i.e., high textural heterogeneity, absence of matrix and biological remains, and non-erosive contacts) and the age of these deposits (1950 AD) suggest a clear anthropogenic influence in the formation of this layer, i.e., debris from management works on the littoral

zone of the lake around this date in order to retain more water (Official Forest Services of São Miguel; Nemésio pers. comm).

Facies S, again represented by a single layer (~1 cm thick) at 29 cm core depth, consists of coarse sand embedded in a matrix of medium sand and silt. Again, this layer might represent an extraordinary flood event that occurred at approximately 1970 AD

4.2.5.- Unit 5 (24 cm to top; ca. 1980 AD to Present)

Unit 5 is composed of massive brown to ochre mud very rich in diatoms dominated by tychoplanktonic Fragilarioid taxa (Facies D). These fine sediments are interbedded with a thin layer of coarse sand (Facies S). Figure 4 shows that the TOC and TN values of Facies D are higher than those of Facies C but lower than those of Facies A and B. However, the TOC MARs are very high, with values similar to those of Facies A. In contrast, the TOC/TN atomic ratio values are the lowest of the sequence, indicating a dominantly algal origin. The amorphous fraction content is also higher than in the other facies (>80 %). It is primarily composed of diatoms and, to a lesser extent, OM and volcanic glass particles. Consequently, this unit presents the lowest mean XRF values of the entire record (Fig. 5). The crystalline fraction is dominated by illite, sanidine and plagioclase, whereas quartz values remain low. The most recent decades of the Lake Empadadas sedimentary record are likely associated with the highest lake levels (Figure 2S Supplementary Material) and lacustrine productivity of the last six centuries, as indicated by the highest TOC MAR values and the presence of very abundant diatoms (mainly belonging to *Fragilaria* s.l.).

4.3.- Main controls of lacustrine sedimentation

Multivariate analyses of the biogeochemical composition of the sediments (i.e., XRF, XRD and OM data) have been performed to recognize the main climatic and geologic controls on lacustrine sedimentation in Lake Empadadas. One of the major problems for this kind of analyses lies in the fact that, in lakes located in volcanic settings, amorphous material can be linked to OM, biogenic silica and/or volcanic glass particles. To overcome this obstacle in Lake Empadadas, the interpretations have been supported by data on the diatom assemblages found in the different facies

The RDA biplot shows three main groups of variables (Fig. 6A): Group A includes data from organic-rich Facies A samples, which are associated with quartz, sanidine and plagioclase. Group B encompasses the amorphous fraction and is mostly related to diatom-rich samples of Facies D. Group C includes K, Mn, Zr, Fe and Si, which are primarily linked to illite, and consists of samples from silty-terrigenous Facies C, volcanic Facies Ta and some of the muddy-silty Facies B. Ca, Sr, Ti and Al are located in the center of the biplot among most of the samples from Facies B

The first two eigenvectors of the PCA account for 82.6 % of the total variance. The first eigenvector (PC1) represents 61.2 % of the total variance and is mainly controlled by all the XRF elements at the negative end and, to a much lesser extent, by TOC and TN at

the positive end (Fig. 6B). The negative values of PC1 are associated with all the chemical elements—particularly Al, Si, Zr, Fe and K—that, in the RDA, are partially positively related to illite (group C) and negatively to the amorphous materials (group B). Analyses show that there is a strong positive relationship between PC1 and Facies D (Fragilarioid diatom-rich) in the PCA, and this facies is related to the amorphous material in the RDA. These data suggest that the origin of the amorphous material in the sedimentary facies of Lake Empadadas is biogenic silica and not the volcanic glass particles, as in the case of volcaniclastic Facies T. Additionally, tychoplanktonic Fragilarioid diatoms (Facies D) are usually characteristic of moderately deep lake conditions, whereas benthic forms, such as the *Cymbella*- and *Pinnularia*-dominated assemblages (Facies C), are typical of near-shore environments (Kingsbury et al., 2012). Furthermore, Facies C (high illite content) and Facies D (low illite content) are on opposite sides of PC1. Thus, the association of higher illite content, lower biogenic silica content and *Cymbella*- and *Pinnularia*-dominated assemblages indicate lower lake levels, whereas the association of lower illite content, higher biogenic silica content and Fragilarioid diatoms indicate higher lake levels. Fluctuations in the lake level mainly reflect changes in precipitation and evaporation integrated over the lakes and their basin catchments. Thus, these fluctuations may constitute a sensitive indicator of past and present climate changes, at least at local and regional scales (Verschuren et al., 2000; Mercier et al., 2002).

The second eigenvector (PC2) accounts for 21 3 % of the total variance and is mainly associated with the TOC and TN concentrations and, to a much lesser extent, with Ti and Ca. In the RDA, TOC and TN belong to group A, which is associated with coarser grain-size minerals, mainly quartz, whereas finer terrigenous materials (illite) are present at its positive end. The TOC and TN amounts are governed by the accumulation of biomass and the subsequent degree of degradation. Consequently, TOC and TN values integrate the different origins of OM, delivery routes, depositional processes, and degree of preservation (Meyers and Teranes, 2001). The burial of OM is frequently followed by a rapid loss of N (Cohen, 2003). However, the nearly parallel behaviors of both the TOC and TN records suggest negligible OM degradation (Fig. 4). Moreover, the origin of OM in the sediments can be characterized by the TOC/TN ratio compositions of algae and vascular plants. Fresh organic matter from phytoplankton has low TOC/TN, whereas vascular land plants have higher TOC/TN ratios (Meyers and Teranes, 2001). Thus, the relationship of this OM to external inputs from the lake catchment, as indicated by the TOC/TN ratio, as well as by the RDA that groups the TOC and TN with coarse siliciclastic minerals, suggests that the PC2 could be interpreted as an indicator of OM accumulation in the sediments from various sources of biogenic origin, autigenic or allochthonous from the catchment. In summary, positive PC2 values indicate greater OM accumulation from several sources and vice versa.

4.4.- Climate and large-scale dynamical forcings

Correlation coefficients among climate variables of the two most important modes of circulation in the Atlantic (as evaluated by Hernández et al., 2016) show that, at a decadal scale, the AMO’s influence over the Azores Archipelago’s precipitation and

temperature is considerably larger than the corresponding NAO impact (Table 2). For the instrumental period (1873-2011; N = 51), the AMO shows significant positive correlations with both temperature and precipitation ($\rho = 0.52$ and $\rho = 0.44$, respectively), whereas the NAO displays a significant negative correlation with precipitation ($\rho = -0.41$) and a positive (but no significant) correlation with temperature. Therefore, at a decadal scale and conversely with the results obtained at a seasonal scale by Hernández et al. (2016), the AMO correlations with the precipitation are higher than those found with the NAO. Thus, despite the NAO influence over Azores climate at seasonal and interannual scales, only AMO exhibits significant statistical correlation at decadal scales with PC1 and PC2 of Lake Empadadas ($\rho = 0.43$ and $\rho = 0.31$, respectively; p-value < 0.05). This suggests a larger influence on the lake level and OM accumulation via climate variables at this longer time scale. Moreover, we can state that the local precipitation and temperature series are positively correlated ($\rho = 0.65$). This is because the precipitation conditions on the Azores Archipelago are positively correlated with the sea surface temperatures around the Archipelago and, therefore, its mean air temperatures (Björck et al., 2006). Precipitation and temperature, in turn, are linked to both major atmospheric patterns of climate variability (i.e., NAO and AMO). Therefore, besides the human activities on the lacustrine catchment, these patterns represent the main driving factors influencing the paleoenvironmental evolution of Lake Empadadas. On one hand, positive (negative) scores of the PC1 are likely linked to high (low) lake levels and mostly high values of both temperature and precipitation. On the other hand, scores of the PC2 are likely associated with OM accumulation modulated by the in-lake primary productivity, the vegetal cover and the precipitation. Summarizing, PC1 is mainly regulated by temperature and precipitation, vegetation density and particle transportation and can be used as a broad indicator of the lake level, whereas PC2 is associated with the OM accumulation and controlled by diverse factors, with the climate and the land uses of the catchment being the most significant (Futter et al., 2008; Mattsson et al., 2015). In addition, both PCs are clearly influenced by the AMO via precipitation and temperature. By contrast, at this time scale (decadal), the NAO influence on the PCs is unclear

5.- Discussion: Lake evolution and environmental impacts

Sedimentological, micropaleontological and geochemical proxy data, as well as the multivariate analysis of these data in terms of origins, have been used to characterize the environmental history of Lake Empadadas recorded in Units 2 to 5. A stratigraphically constrained cluster of data (Figure 3S supplementary material) has allowed us to identify five main stages with environmental significance (Table 3). These stages have been compared to other regional records and the most likely associated forcing factors since ca. 1350 AD

5.1.- Stage 1 (ca. 1350-1450 AD): Intermediate lake levels under a wet and warm climate influenced by a positive AMO

In Lake Empadadas, this stage is defined by positive PC1 values (intermediate lake levels) and the highest PC2 values (very high OM accumulation) (Fig. 7A and B) during

the deposition of Unit 2. This combination of intermediate lake levels and very high allochthonous OM deposition (high TOC/TN values) may correspond to wet and warm climate conditions during the earliest phases of the lake ontogeny, after major volcanic inputs occurred during the deposition of Unit 1.

The Northern Hemisphere temperature reconstruction (Mann et al., 2009) shows that before the onset of the Industrial era, the highest temperatures of the last 1000 years occurred between 1300 AD and 1400 AD (Fig. 7C). Raposeiro et al. (2017) also reported that the latest stages of the warm and arid MCA favored the occurrence of some warmer chironomid taxa in the Lake Azul record (Fig. 7J). These warm conditions were also found elsewhere in southwestern Europe, such as the Ría de Vigo (Álvarez et al., 2005; Muñoz-Sobrino et al., 2014) and Tagus prodelta (Rodrigues et al., 2009). Furthermore, Björck et al (2006) found a change from wet conditions to a drier state during the MCA-LIA transition on Pico Island (Fig. 1 and 7E). Similar wet conditions were reconstructed from sediments in western Iberian settings, such as the Ría de Vigo (Álvarez et al., 2005), the Tagus prodelta (Rodrigues et al., 2009) and the Alboran Sea (Nieto-Moreno et al., 2013). Previous proxy-based AMO and NAO reconstructions presented mainly positive AMO phases and alternating negative and positive NAO phases for these decades (Fig. 7G and H). Our record suggests that warm and wet conditions were caused by a dominant positive AMO phase

5.2.- Stage 2 (ca 1450-1680 AD): Dry and cold climate with very shallow lake levels and negative AMO

Stage 2 corresponds to sediments of the lower part of Unit 3, where PC1 displays lower values (lowstand conditions) and PC2 shows intermediate values (less OM deposition with a larger proportion of material with an in-lake origin compared to that of Stage 1). Thus, the onset of the LIA on São Miguel Island might be characterized by generally cold and dry conditions.

During this stage, Rull et al. (2017) identified human disturbance manifested as local forest burning, cereal cultivation and possibly animal husbandry within the caldera of Sete Cidades, culminating with local deforestation. Arboreal pollen (*Juniperus brevifolia*) nearly disappeared from the Lake Azul record, indicating that native forests were no longer present in the area (Fig. 7I), as was also described in the chronicles of Gaspar Fructuoso (1522-1591) “Saudades da Terra” (Fructuoso, 1977). The dominance of non-arboreal pollen indicates that the vegetation within the neighboring Sete Cidades caldera (Fig. 1) was more open and dominated by native shrubs and grass meadows (Rull et al., 2017), suggesting a recognizable human disturbance of the region (Figures 2S Supplementary Material and 7I). In turn, the first water provision for human uses in this area is documented during the second half of this stage (1512 AD). Therefore, despite the uncertainty of Lake Empadadas basin as the source of this water (Fructuoso, 1977), it can be hypothesized that the lake level drop may have been amplified by these anthropogenic activities

The onset of the LIA is characterized by cold conditions elsewhere in the Northern Hemisphere (Fig. 7C), particularly over the eastern sector of the North Atlantic region (Álvarez et al., 2005; Rodrigues et al., 2009). Nevertheless, there are discrepancies in the interpretation of the past precipitation record. On Pico Island, Björck et al. (2006) defined this stage as a period of transition from dry to wet conditions with a drier LIA onset (Fig. 7E), whereas other North Atlantic and Western Iberia records suggest wetter conditions than in the MCA-LIA transition (Rodrigues et al., 2009; Nieto-Moreno et al., 2013). During the LIA, low solar irradiance promoted the development of frequent and persistent atmospheric blocking events (Moffa-Sánchez et al., 2014). These conditions could have been the main cause of the greater aridity over the Azores Archipelago than over the Iberian Peninsula during this stage, suggesting a more heterogeneous humidity pattern in the North Atlantic area during the LIA onset (Sánchez-López et al., 2016)

For this century the AMO is dominated by negative values, with a clear trend towards the minima of the entire record, whereas the NAO reconstruction mainly shows positive and neutral (NAO ≈ 0) phases, with the exception of negative conditions at ca. 1600 AD coincident with the lowest AMO values (Fig. 7G and H). Nevertheless, a cold and dry climate scenario dominates the whole stage, exhibiting good agreement with the AMO curve pattern. Therefore, the sedimentary infill was dominated by the AMO conditions and likely enhanced and/or modulated by the NAO phase predominance when the influence of the AMO weakened (ca. 1450-1550 AD).

5.3.- Stage 3 (ca. 1680-1850 AD): Wet and warm climate with intermediate lake levels with negative AMO and NAO phases

In Lake Empadadas, the PC1 and PC2 exhibit increasingly positive trends, suggesting a lake level rise and higher OM accumulation throughout Unit 3 (Fig. 7A and B). The vegetation cover of the catchment remains similar to that of the previous stage. However, for the last decades of stage 3 (ca. 1800-1850 AD), the Lake Azul pollen record shows a distinct evolution, with the first appearances of pollen from introduced trees, such as *Pinus pinaster* and *Cryptomeria japonica* (Fig. 7I). This period is likely defined by warm and wet conditions, influenced by negative AMO and a predominantly negative NAO (Fig. 7G and H). The Lake Empadadas record seems to partly disagree with the previous AMO reconstruction (Fig. 7G) and to fit better with the negative NAO signal (Fig. 7H). This could be ascribed to the non-stationary relationship of the large scale modes and the climate variability, in this case when the AMO influence becomes weaker, the NAO other influences appear to increase

The Northern Hemisphere temperature reconstruction (Fig. 7C) and the sedimentary records of the Atlantic margin of the Iberian Peninsula (Álvarez et al., 2005; Rodrigues et al., 2009; Muñoz-Sobrino et al., 2014) display a general increasing trend in temperatures during the second half of the LIA. In terms of humidity, the Alboran Sea recorded a wet-dry-wet pattern during this stage (Nieto-Moreno et al., 2013), whereas the Tagus prodelta sediments (Rodrigues et al., 2009) show a slight increasing trend in the precipitation conditions. In contrast, the precipitation reconstruction from Pico Island

(Lake Caveiro) shows the opposite pattern (Fig. 7E). In this case, it must be stressed that the Lake Caveiro record does not show the same good agreement with the NAO influence as shown during the MCA-LIA transition and the first half of the LIA. This disagreement was explained by the far-from-perfect precipitation-NAO relationship and its non-stationary nature (Björck et al., 2006), which has been described as affecting the NAO-precipitation regime since the 17th century (Pauling et al., 2006; Vicente-Serrano and López-Moreno, 2008). Nevertheless, Sánchez-López et al. (2016) suggested that over the Iberian Peninsula, the distinct regional impact of the climate modes on the meteorological variables could also be explained by the E-W swing of the Azores high-pressure system due to the interaction between the NAO and the East Atlantic pattern. Thus, the disagreement between Pico and São Miguel islands could be similar. However, it should also be acknowledged that the NAO pattern exhibits high interannual variability, which is difficult to identify at this resolution.

5.4.- Stage 4 (ca. 1850-1980 AD): Dry and cold climate with the shallowest lake level influenced by a negative AMO

Unlike in previous stages, measured meteorological observations (precipitation and temperature) and instrumental-based values of NAO and AMO indices are available for this stage. The temperature and precipitation values from Ponta Delgada meteorological station covariate with PC1 and PC2, respectively (Fig. 7A, B, D and F). PC1 shows negative values with a highly oscillating pattern, whereas PC2 experiences an abrupt decrease, with a fairly constant behavior throughout this stage. These patterns indicate colder and wetter conditions than during previous stages, similar to those found on Pico Island (Björck et al., 2006), meaning a dry and cold climate over the Azores Archipelago. In contrast, wet and warm climate patterns were interpreted from Iberian marine records (Álvarez et al., 2005; Rodrigues et al., 2009; Nieto-Moreno et al., 2013). The lake level displayed a decreasing trend during the first half of the deposition of Unit 4, with the lowest values taking place at approximately 1900 AD, coincident with the minimum precipitation for the entire ca. 150-yr-long instrumental record. Afterwards, the lake level rose during the second half of the stage (Unit 4). Oscillations in the lake level at the decadal scale also occurred. In contrast, the OM accumulation remained fairly constant throughout this stage, and the OM was mainly of algal origin (low TOC/TN values), probably because of the consolidated catchment reforestation by the introduction of *Pinus pinaster* and *Cryptomeria japonica* forests beginning at the end of the previous stage (Fig. 7I). The influence of the increased forested catchment most likely buffered the runoff variations, and only the most-intense sandy flood episodes of the entire record were recorded. In addition to these favorable patterns for lowstand conditions, the population growth of the city of Ponta Delgada and its surroundings (Fig. 1B) put pressure on the water resources of São Miguel Island, and the demand for livestock increased (Dias, 1996). Water consumption might therefore have enhanced the lake level drop during the first decades of this stage.

Negative AMO and positive NAO phases dominated the first half of the stage (ca. 1850-1900 AD), resulting in decreases in both precipitation and temperature, which were

reflected in the Lake Empadadas sedimentary record. The period with the lowest precipitation recorded in Ponta Delgada was in the early 1900s, and it is clearly consistent with the Lake Empadadas reconstruction and with the significant negative decadal AMO values. Conversely, the second half of this stage (ca. 1900-1980 AD) experienced a shift toward positive AMO and negative NAO values, leading to higher values of precipitation and temperature (Fig. 7). The persistence of atmospheric blocking conditions between the Iberian Peninsula and the Azores Archipelago controlled by the NAO and East Atlantic pattern during these first decades of the Industrial era (Shabbar et al., 2001; Moffa-Sanchez et al., 2014), as well as the non-stationary interannual NAO influence (Hernández et al., 2016), could again be the main cause of the dry and still cold climate over the Azores Archipelago and the wetter and warmer climate over the Iberian Peninsula.

5.5.- Stage 5 (ca. 1980 AD-Present): Wet and very warm climate with the highest lake levels and very positive AMO

This stage in Lake Empadadas, recorded in sediments of Unit 5, features the highest positive values of PC1 for the entire record, with the PC2 showing low values (Fig. 7A and B). These data therefore indicate the highest lake levels in the studied period, quite similar to the current water depth (Fig. 1). This highstand was favored by the wet scenario recorded on São Miguel Island over the last few decades (Hernández et al., 2016), which was also accompanied by warmer conditions (Cropper and Hanna, 2014). These conditions are also reflected in the increase in warmer chironomid taxa indicators (e.g., *Chironomus plumosus* type) in Lake Azul for the same studied period (Fig. 7J). Wetter and warmer conditions also enhanced the OM accumulation in comparison with the previous stage (Unit 4), although these remained lower than before the reforestation of the catchment (Figures 2S Supplementary Material and 7B). Two extraordinary flood events, indicated by sand layers, occurred in approximately 1976 and 1985 AD. Nevertheless, the highest lake levels in the history of the lake were caused not only by climatic conditions but also by intense anthropogenic activity involving the construction of impermeable works in the littoral zone in 1995 AD by the water council services (SMAS)

Warm and dry conditions have the most common pattern in Western Europe for the last few decades of the Industrial era (e.g., Nieto-Moreno et al., 2013). Nonetheless, some records (e.g., Rodrigues et al., 2009) suggest wetter conditions, similar to the lake records of the Azores (Björck et al., 2006). The predominance of the positive NAO phase (dry conditions) is counteracted by the high positive values of the AMO (wet conditions). Consequently, the amount and intensity of the precipitation has increased over São Miguel Island (Hernández et al., 2016) since the first half of the 20th century. It is worth stressing that the better correlation of the climate variables with the AMO rather than with the NAO suggests that, at decadal to centennial time scales, the AMO mode plays a predominant role, whereas the NAO only modulates the strength of the AMO impact. The previously suggested E-W seesaw of the Azores high-pressure system associated with to the relationship between the NAO and the East Atlantic pattern at interannual time scales could be hypothesized to be responsible for the disagreement between records from the North Atlantic and European sectors

6.- Conclusions

This multiproxy study, based on sedimentological, geochemical and biological proxies, of a sedimentary record from Lake Empadadas has been used to investigate the linkages among sedimentation processes in a lake, the anthropic use of its catchment and decadal climate fluctuations. Multivariate analyses of sediment geochemistry data reveal that two main controls have governed the sedimentary infill. The first control reflects changes in the lake level, whereas the second is related to the variations in the OM accumulation modulated by the anthropic changes in the vegetation of the catchment. In this context, the Lake Empadadas record has provided valuable insights into the climatic and environmental conditions for the last seven centuries for a North Atlantic region lacking sufficient proxy reconstructions despite being located in an ideal sector controlled mostly by the large-scale AMO and NAO modes of variability. In particular, the lake is located in the vulnerable Azores Archipelago system near the southern center of action of the NAO dipole. Despite the contributions of human activities to lake evolution, after a detailed understanding of both in-lake and catchment processes, it has been possible to identify the climatic forces influencing the dynamics of Lake Empadadas. From changes in these two sedimentary controls, five main paleoenvironmental stages have been inferred from ca. 1350 AD to the present: (i) intermediate lake levels and very high OM accumulation (mainly from vascular plants) linked to wet and warm climate conditions dominated by positive AMO phases during the MCA-LIA transition (ca. 1350-1450 AD); (ii) lowstand conditions and intermediate OM deposition related to a dry and cold climate influenced by negative AMO conditions during the first half of the LIA (ca. 1450-1600 AD); (iii) intermediate lake levels and high OM accumulation associated with wet and warm climate conditions controlled by a positive AMO and a predominantly negative NAO during the second half of the LIA (ca. 1600-1850 AD); (iv) the lowest lake level and OM sedimentation (from algal origin) under dry and cold conditions associated with negative AMO phases during the Industrial Era; and (v) the highest lake levels and low algal OM deposition controlled by a wet and very warm climate with very high AMO values between ca. 1980 AD and the present. At decadal to centennial scales, the influence of the AMO on the lake dynamics plays a larger role than the influence of the NAO pattern, which is the main mode of climate variability at the seasonal and interannual time scales. Hence, the decadal to centennial climate variability in this region is predominately influenced by the AMO and is modulated by the NAO when the AMO influence seems lower. We are confident that this result provides a valuable contribution to environmental management, especially for sensitive ecosystems, such as these small oceanic islands representative of Macaronesia in the North Atlantic region, because the AMO presents a longer period and a more predictable evolution than the NAO

Acknowledgments

This work was financed by the Spanish Ministry of Economy and Competitiveness through the PaleoNAO project (CGL2010-15767/BTE) and the RapidNAO project (CGL2013-40608-R). Armand Hernández and Pedro Raposeiro were supported by the Portuguese Science Foundation (FCT) through a post-doctoral grant (SFRH/BPD/79923/2011 and

SFRH/BPD/99461/2014, respectively). The support of the Generalitat de Catalunya to MERS (2014 SGR-1356) is also acknowledged

Figure captions

Figure 1 - A) Map of the Northeastern Atlantic region. Red star indicates the location of Lake Empadadas, and blue circles show the locations of the other records included in this study. B) Map of Azores Archipelago, with an aerial image of Lake Empadadas and its bathymetry. Each contour line corresponds to one meter of depth. The red circle shows the location of Ponta Delgada in São Miguel Island, and the red and yellow stars show the locations of Lake Empadadas and the studied core, respectively. The blue circles show the location of the other records from the Azores Archipelago. C) September 2011 image of Lake Empadadas and its catchment reforested with *Cryptomeria japonica*

Figure 2 - Digital image of core EMN11-04 with sedimentary units, facies, thicknesses and dates. Black and grey arrows indicate radiocarbon dates and ^{210}Pb CF:CS model limits, respectively, in core EMN11-04, and the dates are expressed in calibrated years AD (Table 1). Note that anthropogenic deposits (disorganized gravels) have been removed from the figure

Figure 3 - Age-depth model based on the AMS ^{14}C dates and ^{210}Pb activity-depth profile constructed using the mixed effect regression method (Heegaard et al., 2005). The black continuous line represents the age-depth function framed by the grey lines, which correspond to the error model. Red crosses represent the ^{210}Pb CF:CS model, red circles indicate the AMS ^{14}C radiocarbon dates, and the red triangle denotes the age of the volcanic eruption (P17). Note that sediments considered instantaneous deposits (i.e., anthropogenic deposits) have been removed from the construction of the age model and are represented by the light-grey bands. Corresponding sedimentary units are indicated

Figure 4 - Main organic proxies (main diatom assemblages, elemental compositions of TOC, TOC MAR, TN and TOC/TN ratio) analyzed in the EMN11-04 core. Units, facies and dates are indicated in the column

Figure 5 - Inorganic proxies (selected XRF profiles in thousands of counts per second and XRD results as percentages of the total dry weight) analyzed in the EMN11-04 core. Units, facies and dates are indicated in the column. Note that the XRF data are plotted with a regular spacing of 10 mm to obtain the same spatial resolution of XRD data and to facilitate their comparison

Figure 6 - A) Redundancy Analysis (RDA) biplot for the Lake Empadadas record. Defined groups A, B and C are shown. B) Plot of the plane defined by the first two eigenvectors (PC1 and PC2) obtained via principal component analysis (PCA) of the normalized multiproxy dataset of the Lake Empadadas sediments. In both biplots (A and B), samples of each facies are represented by different colors

Figure 7 - Paleoenvironmental reconstruction based on Lake Empadadas sedimentary sequence. (A) Lake level reconstruction derived from the first PCA eigenvector (PC1)

(present work). (B) Particulate inputs (rough indicator of the runoff modulated by the vegetal cover) derived from the second PCA eigenvector (PC2) (present work). (C) Northern Hemisphere proxy-based temperature reconstruction (Mann et al., 2009). (D) Instrumental measured temperature (1873-2011) from Ponta Delgada. The black line represents annual data, and the red line represents an 11-point moving mean (Cropper and Hanna, 2014). (E) Precipitation reconstruction from Lake Caveiro (Pico Island, Azores Archipelago) based on the sedimentary record (Björck et al., 2006). (F) Instrumental measured precipitation record (1873-2012) from Ponta Delgada. The black line represents annual data, and the blue line represents an 11-point moving mean (Hernández et al., 2016). (G) Combined instrumental (1856-2011), calculated (NOAA data), and proxy-based reconstruction (Mann et al., 2009) of the AMO (shaded areas correspond to the proxy-based reconstruction during the instrumental period). (H) Combined instrumental (1850-2011), calculated (Cropper et al., 2015), and proxy-based reconstruction (Ortega et al., 2015) of the NAO (shaded areas correspond to the proxy-based reconstruction during the instrumental period). (I) Arboreal vs. non-arboreal pollen records from the sedimentary sequence of Lake Azul (São Miguel Island, Azores Archipelago) (Rull et al., 2017). (J) Summary of the main chironomid taxa from the Lake Azul record (Raposeiro et al., 2017). All data are plotted against age. Grey bands indicate time periods with no data

Table 1 - Radiocarbon dates and calibrated ages for the EMN11-04 core.

Table 2: Multiannual Spearman's rank correlation coefficients during the instrumental period (1873-2011; N=51). Grey, regular and bold numbers indicate values at $p > 0.05$, $p < 0.05$ and $p < 0.01$, respectively. Confidence levels were computed assuming a Gaussian distribution of errors. PREi: Precipitation instrumental data from Ponta Delgada meteorological station; TEMPi: Temperature instrumental data from Ponta Delgada meteorological station; NAOi: North Atlantic Oscillation index values for instrumental data obtained from Cropper et al. (2015); and AMOi:. Atlantic Multidecadal Oscillation index values for instrumental period obtained from the NOAA database

Table 3 - Summary of the main paleoenvironmental characteristics for each defined paleoclimate stage

References

Álvarez MC, Flores JA, Sierro FJ, Diz P, Francés G, Pelejero C, Grimalt J. 2005. Millennial surface water dynamics in the Ría de Vigo during the last 3000 years as revealed by coccoliths and molecular biomarkers. Palaeogeography. Palaeoclimatology. Palaeoecololgy 218, 1–13. doi:10 1016/j palaeo 2004 12 002

Andrade C, Trigo RM, Freitas MC, Gallego MC, Borges P, Ramos AM. 2008. Comparing historic records of storm frequency and the North Atlantic Oscillation (NAO) chronology for the Azores region. Holocene 15, 745–754. doi org/10 1177/0959683608091794

Azevedo JMM, Ferreira MP. 2006. The volcanotectonic evolution of Flores Island, Azores (Portugal). Journal of Volcanology and Geothermal Research 156, 90-102. doi org/10 1016/j jvolgeores 2006 03 011

Bennett KD. 1996. Determination of the number of zones in a biostratigraphical sequence. New Phytologist 132, 155–170. doi:10 1111/j 1469-8137 1996 tb04521 x

Bradley RS, Jones PD. 1992. Records of explosive volcanic eruptions over the last 500 years. In: Climate Since AD 1500, Bradley RS, Jones PD (eds). Routledge: London.

Broecker WS. 2000. Was a change in thermohaline circulation responsible for the Little Ice Age? Proceedings of the National Academy of Sciences of the United States of America 97, 1339-1342. doi: 10 1073/pnas 9741339

Björck S, Rittenour T, Rosén P, França Z, Möller P, Snowball I, Wastegård S, Bennike O, Kromer B. 2006. A Holocene lacustrine record in the central North Atlantic: proxies for volcanic activity, short-term NAO mode variability, and long-term precipitation changes. Quaternary Science Reviews 25, 9–32. doi: 10 1016/j quascirev200508008

Chung FH. 1974a. Quantitative interpretation of X-ray diffraction patterns of mixtures. I. Matrixflushing method for quantitative multicomponent analysis. Journal of Applied Crystallography 7, 519–525

Chung FH. 1974b. Quantitative interpretation of X-ray diffraction patterns of mixtures. II. Adiabatic principle of X-ray diffraction analysis of mixtures. Journal of Applied Crystallography 7, 526–531

Cohen AS. 2003. Paleolimnology: the History and Evolution of Lake Systems. Oxford University, Press, p. 528

Conroy JL, Overpeck JT, Cole JE, Shanahan TM, Steinitz-Kannan M. 2008. Holocene changes in eastern tropical Pacific climate inferred from a Galápagos lake sediment record. Quaternary Science Reviews 27, 1166-1180. doi: 101016/j quascirev 200802015

Cropper TE, Hanna E. 2014. An analysis of the climate of Macaronesia, 1865–2012. International Journal of Climatology 34, 604–622, doi: 101002/joc 3710

Cropper T, Hanna E, Valente MA, Jónsson T. 2015. A daily Azores–Iceland North Atlantic Oscillation index back to 1850. Geoscience Data Journal 2, 12–24. doi: 101002/gdj323

Cruz JV, Antunes P, Amaral C, França Z, Nunes JC. 2006. Volcanic lakes of the Azores archipelago (Portugal): Geological setting and geochemical characterization. Journal of Volcanology and Geothermal Research 156, 135-157.

Dias E. 1996. Ponta Delgada 450 Anos de Cidade. Jornal de Cultura,. Ponta Delgada, Portugal. pp. 136.

Fischer EM , Luterbacher J,. Zorita E,. Tett SFB,. Casty C, Wanner H. 2007. European climate response to tropical volcanic eruptions over the last half millennium, Geophysical Research Letters 34, L05707, doi:10 1029/2006GL027992

Fructuoso G. 1977. Livro Quarto das Saudades da Terra. Instituto Cultural de Ponta Delgada, Ponta Delgada.

Futter MN, Starr M, Forsius M, Holmberg M. 2008. Modelling the effects of climate on long-term patterns of dissolved organic carbon concentrations in the surface waters of a boreal catchment. Hydrology and Earth System Sciences 12, 437-447. doi:10 5194/hess-12-437-2008

Giralt S, Moreno A, Bao R, Sáez A, Prego R, Valero-Garcés BL, Pueyo JJ, González-Sampériz P, Taberner C. 2008. A statistical approach to disentangle environmental forcings in a lacustrine record: the Lago Chungara case (Chilean Altiplano). Journal of Paleolimnology 40, 195–215. doi:10 1007/s10933-007-9151-9

Heegaard E, Birks HJB, Telford RJ. 2005. Relationships between calibrated ages and depth in stratigraphical sequances: an estimation procedure by mixed-effect regression. The Holocene 15, 612-618. doi: 10 1191/0959683605hl836rr

Hernández A, Kutiel H, Trigo RM, Valente MA, Sigró J, Cropper T, Santo FE. 2016. New Azores archipelago daily precipitation dataset and its links with large-scale modes of climate variability. Interantional Journal of Climatology 36, 4439–4454. doi:10 1002/joc 4642

Hochberg Y. 1988. A sharper Bonferroni procedure for multiple tests of significance. Biometrika 75, 800–802. doi: 10 1093/biomet/75 4 800

Hurrell JW. 1995. Decadal trends in the North Atlantic Oscillation and relationship to regional temperature and precipitation. Science 269, 676–679.

Hurrell JW, Kushnir Y, Ottersen G, Visbeck M. 2003. An overview of the North Atlantic Oscillation. In: Hurrell, J W , Kushnir, Y , Ottersen, G , Visbeck, M. (Eds). The North Atlantic Oscillation. Climatic Significance and Environmental Impact. American Geophysical Union, Washington, pp. 1-35.

IPCC. 2014. Climate Change 2014: Mitigation of Climate Change. Contribution of Working Group III to the Fifth Assessment Report of the Intergovernmental Panel on Climate Change, Edenhofer O, Pichs-Madruga R, Sokona Y, Farahani E, Kadner S, Seyboth K, Adler A, Baum I, Brunner S, Eickemeier P, Kriemann B, Savolainen J, Schlömer S, von Stechow C, Zwickel T, Minx JC (eds). Cambridge University Press: London and New York, NY.

Jerez S, Trigo RM. 2013. Time-scale and extent at which large-scale circulation modes determine the wind and solar potential in the Iberian Peninsula. Environmental Research Letters 8, 044035. doi: 10 1088/1748-9326/8/4/044035

Jones PD, Briffa KR, Osborn TJ, Lough JM, Van Ommen TD, Vinther BM, Luterbacher J, Wahl ER, Zwiers FW, Mann ME, Schmidt GA, Ammann CM, Buckley BM, Cobb KM, Esper J, Goosse H, Graham N, Jansen E, Kiefer T, Kull C, Küttel M, Mosley-Thompson E, Overpeck JT, Riedwyl N, Schulz M, Tudhope AW, Villalba R, Wanner H, Wolff E, Xoplaki E. 2009. High-resolution palaeoclimatology of the last millennium: a review of current status and future prospects. The Holocene 19, 3-49. doi:10.1177/0959683608098952

Kienel U, Schwab MJ, Schettler G. 2005. Distinguishing climatic from direct anthropogenic influences during the past 400 years in varved sediments from Lake Holzmaar (Eifel, Germany). Journal of Paleolimnology 33, 327-347. doi:10.1007/s10933-004-6311-z

Kingsbury MV, Laird KR, Cumming BF. 2012. Consistent patterns in diatom assemblages and diversity measures across water-depth gradients from eight Boreal lakes from north-western Ontario (Canada). Freshwater Biology 57, 1151-1165. doi: 10.1111/j.1365-2427.2012.02781.x

Kossin JP, Camargo SJ, Sitkowski M. 2010. Climate modulation of North Atlantic hurricane tracks. Journal of Climate 23, 3057–3076. doi: 10.1175/2010JCLI3497.1

Madeira J. 2007. A erupção dos Capelinhos e o Vulcanismo nos Açores. Boletim do Núcleo Cultural da Horta 16, 29-44.

Mann ME, Zhang Z, Rutherford S, Bradley RS, Hughes MK, Shindell D, Ammann C, Faluvegi G, Ni F. 2009. Global Signatures and Dynamical Origins of the Little Ice Age and Medieval Climate Anomaly. Science 326, 1256-1260. doi: 10.1126/science.1177303.

Margalef O, Cañellas-Boltà N, Pla-Rabes S, Giralt S, Pueyo JJ, Joosten H, Rull V, Buchaca T, Hernández A, Valero-Garcés BL, Moreno A, Sáez A. 2013. A 70,000 year multiproxy record of climatic and environmental change from Rano Aroi peatland (Easter Island). Global and Planetary Change 108, 72–84. doi: 10.1016/j.gloplacha.2013.05.016

Marshall J, Kushner Y, Battisti D, Chang P, Czaja A, Dickson R, Hurrell J, McCartney M, Saravanan R, Visbeck M. 2001. North Atlantic climate variability: phenomena, impacts, and mechanisms. International Journal of Climatology 21, 1863–1898. doi: 10.1002/joc.693

Mattsson T, Kortelainen P, Räike A, Lepistö A, Thomas DN. 2015. Spatial and temporal variability of organic C and N concentrations and export from 30 boreal rivers induced by land use and climate. Science of Total Environment 508, 145–154. doi: 10.1016/j.scitotenv.2014.11.091.

Mercier F, Cazenave A, Maheu C. 2002. Interannual lake level fluctuations (1993–1999) in Africa from Topex/Poseidon: connections with ocean–atmosphere interactions over the Indian Ocean. Global and Planetary Change 32, 141-163. doi: 10.1016/S0921-8181(01)00139-4

Meyers, P A , Teranes, J L , 2001. Sediment organic matter, in: Smol, J P , Birks, H J B , Last, W M. (Eds), Tracking Environmental Change Using Lake Sediments. Volume 2: Physical and Geochemical Methods. Kluwer Academic Publishers, Dordrecht, pp. 239-269

Moffa-Sánchez P, Born A, Hall IR, Thornalley DJR, Barker S. 2014. Solar forcing of north Atlantic surface temperature and salinity over the past millennium. Nature Geosciences 7, 275-278. doi:10.1038/ngeo2094

Moore R. 1991. Geology of the three late quaternary stratovolcanoes on São Miguel, Azores. U S. Geol. Surv. Bull. 1900. 46 pp

Moore RB, Rubin M. 1991. Radiocarbon dates for lavaflows and pyroclastic deposits on São Miguel, Azores. Radiocarbon 33, 151–164.

Moreira JM, 1987. Alguns aspectos de intervenção humana na evolução da paisagem da ilha de S. Miguel (Açores). Serviço Nacional de Parques, Reservas e Conservação da Natureza, Lisboa

Muñoz-Sobrino C, García-Moreiras I, Castro Y, Martínez Carreño N, de Blas E, Fernandez Rodríguez C, Judd A, García-Gil S. 2014. Climate and anthropogenic factors influencing an estuarine ecosystem from NW Iberia: new high resolution multiproxy analyses from San Simon Bay (Ría de Vigo). Quaternary Science Reviews 93, 11-33. doi:10 1016/j quascirev 2014 03 021

Nieto-Moreno V, Martinez-Ruiz F, Giralt S, Gallego-Torres D, Garcia-Orellana J, Masqué P, Ortega-Huertas M. 2013. Climate imprints during the ‘Medieval Climate Anomaly’ and the ‘Little Ice Age’ in marine records from the Alboran Sea basin. Holocene 23, 1227-1237. doi: 10.1177/0959683613484613

Nurse LA, McLean RF, Agard J, Briguglio LP, Duvat-Magnan V, Pelesikoti N, Tompkins E, Webb A. 2014. Small islands. In: Climate Change 2014: Impacts, Adaptation, and Vulnerability. Part B:Regional Aspects. Contribution of Working Group II to the Fifth Assessment Report of the Intergovernmental Panel on Climate Change, Barros VR, Field CB, Dokken DJ, Mastrandrea MD, Mach KJ, Bilir TE, Chatterjee M, Ebi KL, Estrada YO, Genova RC, Girma B, Kissel ES, Levy AN, MacCracken S, Mastrandrea PR, White LL (eds). Cambridge University Press: London and New York, NY, 1613–1654.

Ortega P, Lehner F, Swingedouw D, Masson-Delmotte V, Raible CC, Casado M, Yiou P. 2015. A model-tested North Atlantic Oscillation reconstruction for the past millennium. Nature 523, 71-74.

Ottersen G, Planque B, Belgrano A, Post E, Reid PC, Stenseth N C. 2001. Ecological effects of the North Atlantic oscillation. Oecologia 128, 1-14.

PAGES 2k Consortium, 2013. Continental-scale temperature variability during the past two millennia. Nature Geosciences 6, 339-346. doi:10.1038/ngeo1797

Pauling A, Luterbacher J, Casty C, Wanner H. 2006. 500 years of gridded high-resolution precipitation reconstructions over Europe and the connection to large-scale circulation. Climate Dynamics 26, 387–405. doi:10 1007/s00382-005-0090-8

Pereira CL, Raposeiro PM, Costa AC, Bao R, Giralt S, Gonçalves V. 2014. Biogeography and lake morphometry drive diatom and chironomid assemblages' composition in lacustrine surface sediments of oceanic islands. Hydrobiologia 730, 93-112.

Porteiro J. 2000. Lagoas dos Açores: elementos de suporte ao planeamento integrado. PhD thesis. University of the Azores. Portugal.

Queiroz G, Pacheco JM, Gaspar JL, Aspinall WP, Guest JE, Ferreira T. 2008. The last 5000 years of activity at Sete Cidades volcano (São Miguel Island, Azores): Implications for hazard assessment. Journal of Volcanology and Geothermal Research 178, 562-573. doi: 10.1016/j.jvolgeores.2008.03.001

R Development Core Team, 2015. R: A Language and Environment for Statistical Computing. R Foundation for Statistical Computing, Vienna, Austria http://www R-project org

Raposeiro PM, Rubio-Inglés MJ, González A, Hernández A, Vázquez-Loureiro D, Rull V, Bao R, Costa AC, Gonçalves V, Sáez A, Giralt S. 2017. Impact of the historical introduction of exotic fishes on chironomid community of Lake Azul (Azores Islands) and relevance for paleolimnological reconstruction. Palaeogeography. Palaeoclimatology. Palaeoecololgy, 77–88. doi:10 1016/j palaeo 2016 11 015

Reimer PJ, Bard E, Bayliss A, Beck JW, Blackwell PG, Ramsey CB, Buck CE, Cheng H, Edwards RL, Friedrich M, Grootes PM, Guilderson TP, Haflidason H, Hajdas I, Hatté C, Heaton TJ, Hoffmann DL, Hogg AG, Hughen KA, Kaiser KF, Kromer B, Manning SW, Niu M, Reimer RW, Richards DA, Scott EM, Southon JR, Staff RA, Turney CSM, van der Plicht J. 2013. IntCal13 and Marine13 Radiocarbon Age Calibration Curves 0–50,000 Years cal BP. Radiocarbon 55, 1869-1887. doi: 10.2458/azu_js_rc.55.16947

Robbins JA. 1978. Geochemical and geophysical applications of radioactive lead. The biogeochemistry of lead in the environment 1, 285-405.

Rodrigues T, Grimalt JO, Abrantes FG, Flores JA, Lebreiro SM. 2009. Holocene interdependences of changes in sea surface temperature, productivity, and fluvial inputs in the Iberian continental shelf (Tagus mud patch). Geochemistry Geophysics Geosystems 10. doi:10 1029/2008GC002367

Rull V, Lara A, Rubio-Inglés MJ, Giralt S, Gonçalves V, Raposeiro P, Hernández A, Sánchez G, Vázquez-Loureiro D, Bao R, Masqué P, Sáez A. 2017. Vegetation changes, lake-level variations and human pressure in the caldera of Sete Cidades (São Miguel, Azores Islands) during the last 700 years: the lake Azul pollen record. Quaternary Science Reviews 159, 155-168. doi:10 1016/j quascirev 2017 01 021

Sánchez-Cabeza J A, Masqué P, Ani-Ragolta I. 1998. Pb-210 and Po-210 analysis in sediments and soils by microwave acid digestion. Journal of Radioanalytical and Nuclear Chemistry 227, 19–22.

Sánchez-López G, Hernández A, Pla-Rabes S, Trigo RM, Toro M, Granados I, Sáez A, Masqué P, Pueyo JJ, Rubio-Inglés MJ, Giralt S. 2016. Climate reconstruction for the last two millennia in central Iberia: The role of East Atlantic (EA), North Atlantic Oscillation (NAO) and their interplay over the Iberian Peninsula. Quaternary Science Reviews 149, 135–150. doi:10 1016/j quascirev 2016 07 021

Santos FD, Valente MA, Miranda PMA, Aguiar A, Azevedo EB, Tome AR, Coelho F. 2004. Climate change scenarios in the Azores and Madeira Islands. World Resources. Review 16, 473–491.

Shabbar A, Huang J, Higuchi K. 2001. The relationship between the wintertime north Atlantic oscillation and blocking episodes in the north Atlantic. International Journal of Climatology 21, 355–369. doi: 10.1002/joc.612

Shindell DT, Schmidt GA, Mann ME, Rind D, Waple A. 2001. Solar forcing of regional climate change during the Maunder Minimum. Science 294, 2149–2152. doi: 10.1126/science.1064363

Shotton FW, Williams REG. 1971. Birmingham University Radiocarbon dates III. Radiocarbon 11, 266.

Stuiver M, Reimer PJ. 1993. Extended C-14 data base and revised Calib 3 0 C-14 age calibration program. Radiocarbon 35, 215–230.

Sutton RT, Hodson D L. 2005. Atlantic Ocean forcing of North American and European summer climate. Science 309, 115-118. doi: 10.1126/science.1109496

Terry RD, Chillingar GV. 1955. Summary of "Concerning some additional aids in studying formations" by MS Shvetsov. Journal of Sedimentary Petrology 25, 229–234.

Trigo RM, Pozo-Vazquez D, Osborn TJ, Castro-Diez Y, Gámis-Fortis S, Esteban-Parra MJ. 2004. North Atlantic Oscillation influence on precipitation, river flow and water resources in the Iberian peninsula. International Journal of Climatology 24, 925–944. doi: 10 1002/joc 1048

Trouet V, Scourse JD, Raible CC. 2012. North Atlantic storminess and Atlantic Meridional Overturning Circulation during the last Millennium: Reconciling contradictory proxy records of NAO variability. Global and Planetary Change 84, 48-55. doi: 10.1016/j.gloplacha.2011.10.003

Vaquero JM, Trigo RM. 2015. Redefining the limit dates for the Maunder minimum. New Astronomy 34, 120-122. doi: 10.1016/j.newast.2014.06.002

Verschuren D, Laird KR, Cumming BF. 2000. Rainfall and drought in equatorial east Africa during the past 1,100 years. Nature 403, 410-414. doi:10.1038/35000179

Vicente-Serrano SM, López-Moreno JI. 2008. The nonstationary influence of the North Atlantic Oscillation on European precipitation. Journal of Geophysical Research Atmospheres 113:,D20120. doi:10 1029/2008JD010382

Volkov DL, Fu L-L. 2010. On the reasons for the formation and variability of the Azores Current. Journal of Physical Oceanography 40, 2197-2220. doi: 10 1175/2010JPO4326 1

Yamamoto A , Palter JB. 2016. The absence of an Atlantic imprint on the multidecadal variability of wintertime European temperature. Nature communications 7. doi:10 1038/ncomms10930

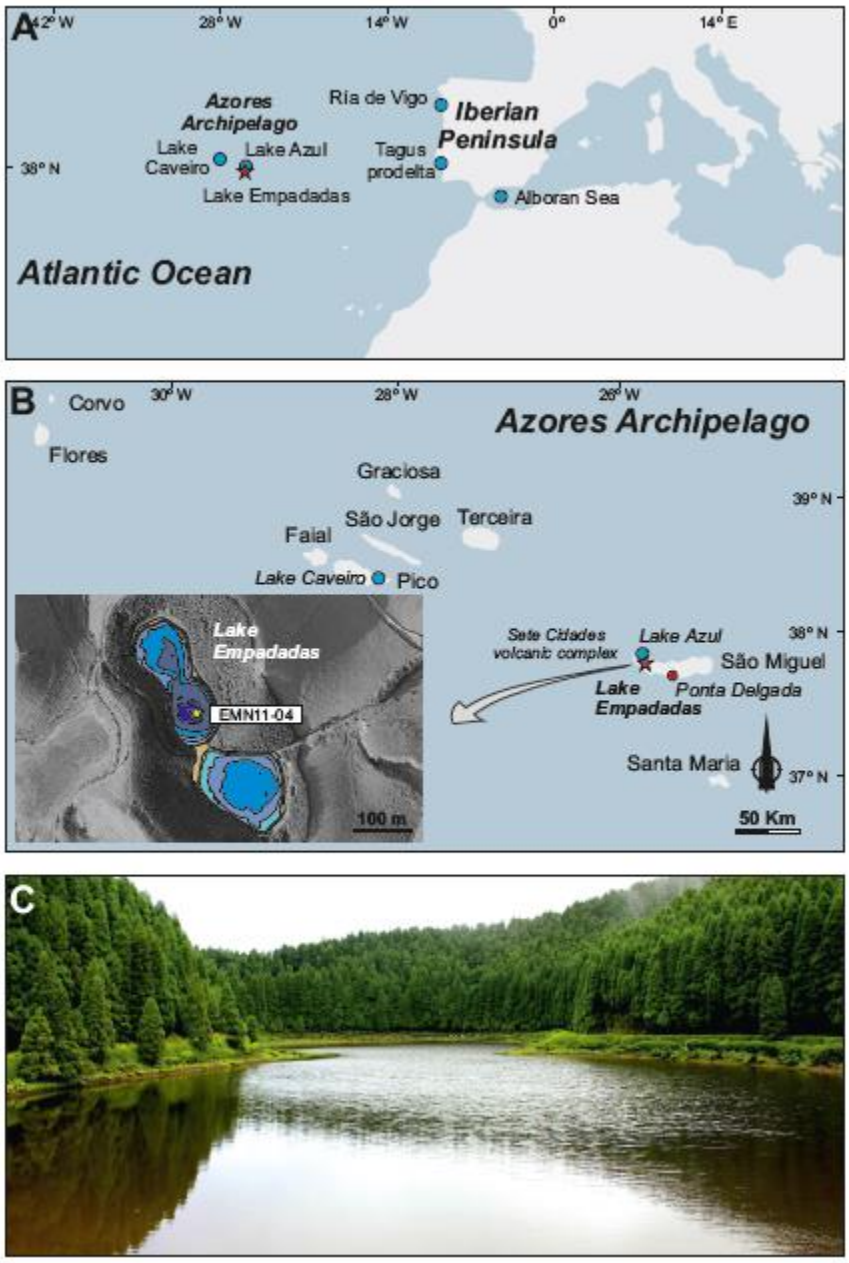

Figure 1

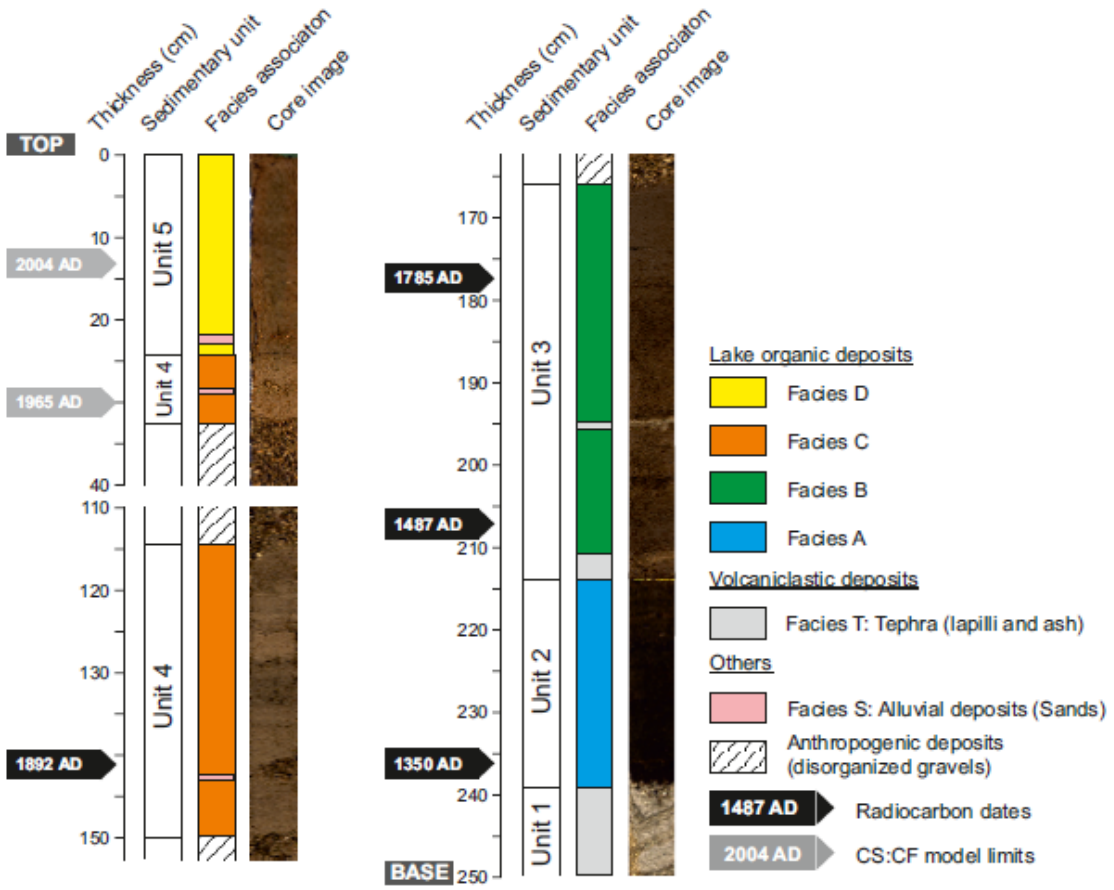

Figure 2

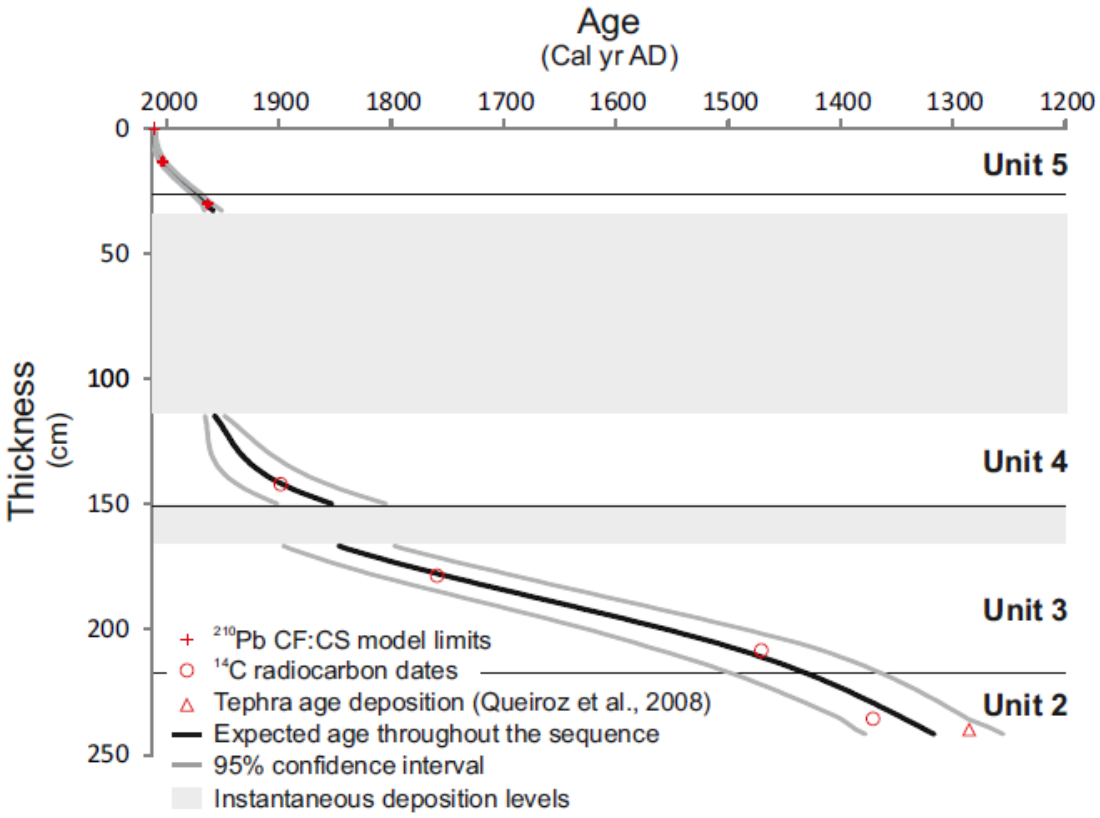

Figure 3

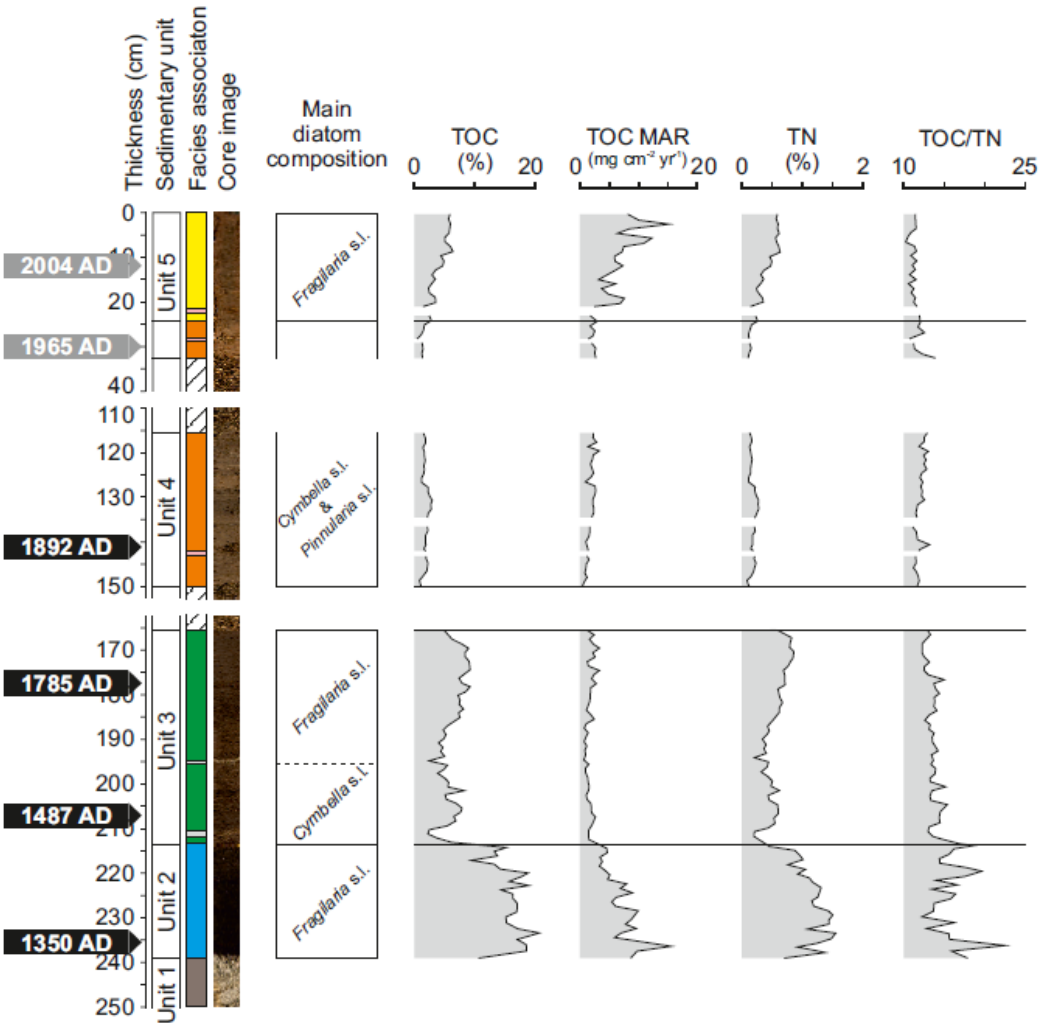

Figure 4

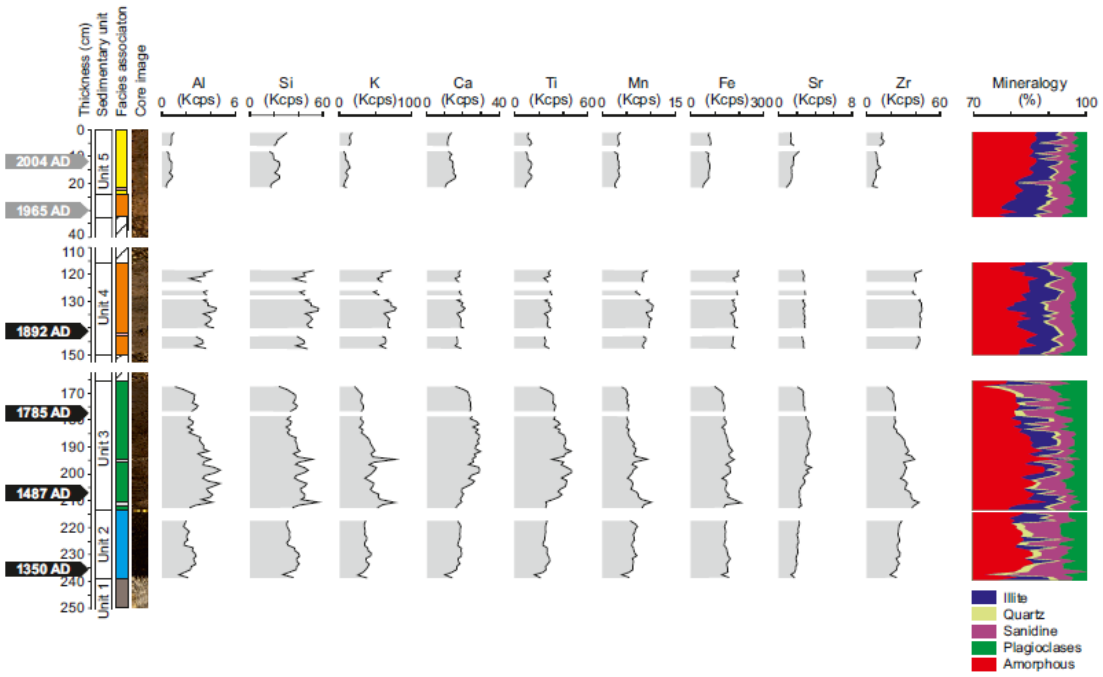

Figure 5

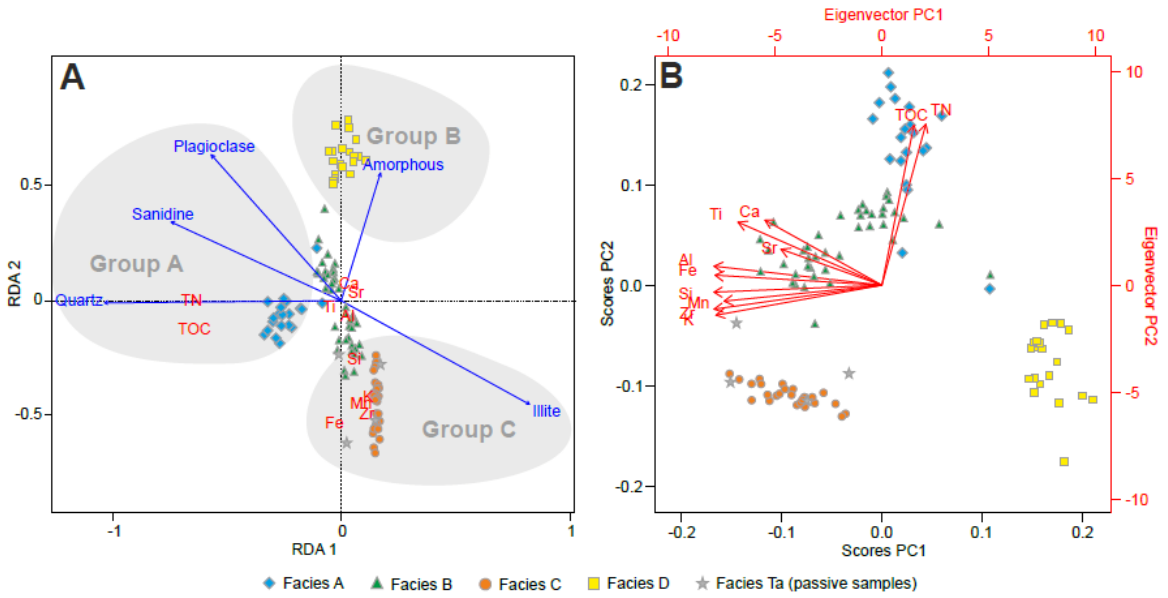

Figure 6

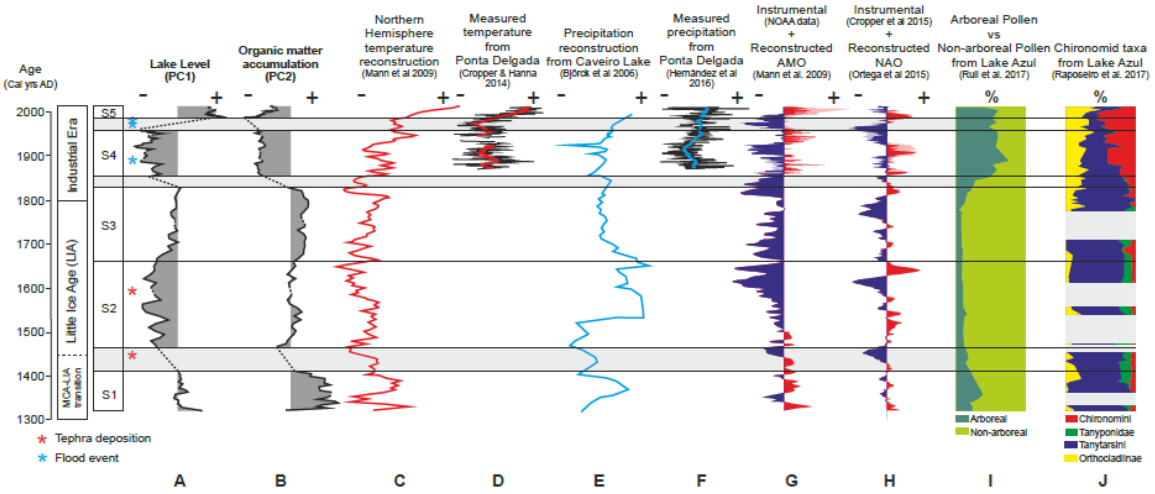

Figure 7

Sample reference	Lab ID	Depth (cm)	$\delta^{13}C$ (‰)	Measured Age ^{14}C (years BP)	Median probability (cal yrs AD)	2σ (cal yrs AD)
EMN11/04/02-54	Beta-316589	141.5	-25.7	50 ± 30 BP	1892	1866 - 1918
EMN11/04/02-90	Beta-333756	177.5	-26.9	150 ± 30 BP	1785	1717 - 1783
EMN11/04/02-119.5	Beta-316590	207	-27.8	390 ± 30 BP	1487	1441 - 1523
EMN11/04/03-23	Beta-316591	236.5	-28.2	630 ± 30 BP	1350	1337 - 1398

Note: ^{210}Pb dates -> CF:CS model, 2 sections: 0-13 cm: 2.0±0.7 cm/y; 13-30 cm: 0.43±0.04 cm/y

Table 1.- Radiocarbon dates and calibrated ages for the EMN11-04 core.

N=51	PC1	PC2	PREi	TEMPi	NAOi	AMOi
PC1	1					
PC2	0.22	1				
PREi	**0.51**	**0.58**	1			
TEMPi	**0.69**	0.47	**0.65**	1		
NAOi	0.05	-0.02	-0.41	0.15	1	
AMOi	0.43	0.31	**0.44**	**0.52**	-0.24	1

Table 2: Multiannual Spearman's rank correlation coefficients during the instrumental period (1873-2011; N=51). Grey, regular and bold numbers indicate values at $p > 0.05$, $p < 0.05$ and $p < 0.01$, respectively.

	Sedimentary unit	***Lake water level***	***Organic matter accumulation***	***Vegetation cover***	***Humidity conditions***	***Thermal conditions***	***AMO phase***	***NAO phase***
Stage 5 (c. 1980 AD-Present)	Unit 5	Highstand	Low	Trees	Wet	Very Warm	Very Positive	Positive
Stage 4 (c. 1850 - 1980 AD)	Unit 4	Lowstand	Very low	Trees	Dry	Cold	Negative	Positive
Stage 3 (c. 1680 - 1850 AD)	Unit 3	Intermediate	High	Shrubs	Wet	Warm	Negative	Negative
Stage 2 (c. 1450 - 1680 AD)	Unit 3	Lowstand	Intermediate	Shrubs	Dry	Cold	Negative	Positive
Stage 1 (c. 1350 - 1450 AD)	Unit 2	Intermediate	Very High	Trees and Shrubs	Wet	Warm	Positive	Neutral

Table 3.- Summary of the main paleoenvironmental characteristics for each defined paleoclimate stage.

Highlights

- We conduct a multiproxy environmental reconstruction from Azorean lake sediments.
- Lake sedimentation was principally governed by climate variability.
- Catchment changes controlled by human activities modulated the climate impact.
- The AMO plays a larger role than the NAO on the lake dynamics at decadal scale.
- The NAO is the main mode influencing the lake variability at subdecadal scales.